Clays and Clay Minerals, Vol. 42, No. 6, 737–746, 1994.

FERRIHYDRITE: SURFACE STRUCTURE AND ITS EFFECTS ON PHASE TRANSFORMATION

JIANMIN ZHAO, FRANK E. HUGGINS, ZHEN FENG, AND GERALD P. HUFFMAN

The Consortium for Fossil Fuel Liquefaction Science, 341 Bowman Hall, University of Kentucky
Lexington, Kentucky 40506

Abstract—X-ray absorption fine structure (XAFS) spectra were collected on a series of ferrihydrite samples prepared over a range of precipitation and drying conditions. Analysis of the XAFS pre-edge structures shows clear evidence of the presence of lower coordination sites in the material. These sites, which are most likely tetrahedral, are believed to be at the surface and become coordination unsaturated (CUS) after dehydroxylation. With chemisorbed water molecules, the CUS sites become the crystal growth sites responsible for the phase transformation of ferrihydrite to hematite at low temperatures. On the other hand, when impurity anions such as SiO_4^{-4} are present in the precipitation solution, the CUS sites may instead absorb the impurity anions, thereby blocking the crystal growth sites and inhibiting the formation of hematite.

Key Words—Ferrihydrite, Mössbauer spectroscopy, Phase transformation, Surface structure, X-ray absorption fine structure (XAFS).

INTRODUCTION

Ferrihydrite is a natural occurring material and can be synthesized by rapid hydrolysis of Fe(III) solution. It is regarded as one of the eight major iron oxide/oxyhydroxides (Schwertmann and Cornell 1991). The structure of ferrihydrite, however, is still a subject of controversy. Because of its poor crystallinity, X-ray diffraction shows a very broad 2-line or 6-line pattern, which makes it difficult to obtain accurate structural information. A number of formulae have been proposed such as $5Fe_2O_3 \cdot 9H_2O$ (Fleischer *et al* 1975), $Fe_5HO_8 \cdot 4H_2O$ (Towe and Bradley 1967), and $Fe_2O_3 \cdot 2FeOOH \cdot 2.6H_2O$ (Russell 1979). These formulae are essentially equivalent and can be reduced to $FeOOH \cdot 0.4H_2O$, i.e., a hydrated iron oxyhydroxide formula.

The average particle size of ferrihydrite is unusually small (~30 Å). In determining the structure of nanoscale materials, consideration must be afforded as much to the surface as to the interior of the particle because the surface constitutes a considerable fraction of the total volume. Assuming the ferrihydrite particle is spherical and the thickness of the surface layer is ~2 Å (equivalent to the Fe^{3+}–O bond distance), the surface region thus comprises >30% of the total volume; any particle shape deviating from spherical would increase the surface fraction. The stoichiometry of a surface is generally different from that of the interior. For example, the surface layer of γ-Al_2O_3 usually consists of OH groups instead of oxygens (Knözinger and Ratnasamy 1978). In addition, since the surface is exposed to the environment, the surface stoichiometry is influenced by temperature, humidity, chemisorption, and other factors. Therefore, one formula would not be adequate to describe the whole structure of a nanoscale particle.

The surface of ferrihydrite plays a role in the phase transformation of ferrihydrite to crystalline hematite (α-Fe_2O_3) and goethite (α-FeOOH). The phase transformation rate depends on the surface water content as well as temperature (Schwertmann and Cornell 1991; Johnston and Lewis 1983). It is retarded by chemisorbed species such as organics, phosphate, and silicate (Schwertmann and Thalmann 1979; Karim 1984; Quin *et al* 1988).

Because of its reactivity and large specific surface area (>200 m^2/g), ferrihydrite is a good adsorbent in aquatic systems (Waychunas *et al* 1993; Fuller *et al* 1993). It has also been studied as a catalyst for a number of reactions (Liaw *et al* 1989, identified as amorphous FeOOH). We have recently investigated the structure and coal liquefaction activity of a commercial ferrihydrite catalyst (NANOCAT) provided by Mach I, Inc. (340 East Church Road, King of Prussia, PA 19406) (Huffman *et al* 1993; Zhao *et al* 1993; Feng *et al* 1993). The catalyst was originally identified as α-Fe_2O_3 by the manufacturer. Using X-ray absorption fine structure (XAFS) spectra, we found that the bulk structure of the material is FeOOH-like with an octahedral symmetry. However, a significant percentage of iron ions at the surface are in the lower coordination sites and they become coordination unsaturated (CUS) after dehydroxylation (Zhao *et al* 1993). Previously, with XAFS spectra collected on a laboratory EXAFS facility equipped with a rotating anode as the X-ray source, Eggleton and Fitzpatrick (1988) claimed that as many as 35% of the iron ions in ferrihydrite are in the tetrahedral sites. Their conclusion was disputed by Manceau *et al* (1990) on the basis of the XAFS spectra collected at synchrotron radiation facilities. The presence of tetrahedral sites in ferrihydrite has also been a

Copyright © 1994, The Clay Minerals Society

https://doi.org/10.1346/CCMN.1994.0420610 Published online by Cambridge University Press

controversial subject in the interpretation of the Mössbauer spectra (Cardile 1988; Murad 1988; Pankhurst and Pollard 1992).

In this study, the structure of ferrihydrite was investigated in detail using XAFS spectroscopy for a series of ferrihydrite samples synthesized over a range of precipitation and drying conditions. X-ray diffraction (XRD) and Mössbauer spectroscopy were used as supplemental techniques for phase characterization, while the morphologies of the samples were examined by transmission electron microscope (TEM). In addition to pure ferrihydrite, ferrihydrite samples with chemisorbed Al and Si were synthesized and the effects of chemisorption on phase transformation of ferrihydrite to hematite were studied using XRD.

EXPERIMENTAL METHODS

Sample preparation

Six ferrihydrite samples were prepared as follows. 1. 2-line ferrihydrite (FHYD I) provided by Mach I, Inc. (NANOCAT). The material was flame synthesized from iron carbonyl at 500°C in a moisture-free environment and has been used for enhancing the combustion rate of rocket fuel (Rudy and Goodson 1991). It is a free-flowing, reddish-brown powder with bulk density (measured without pressing) of only 0.08 g/cm^3, which is one tenth of the bulk densities of the lab synthesized ferrihydrite samples. The material may absorb as much as 15% by weight of water upon prolonged exposure to moist air. To avoid air exposure, the sample was stored under N_2 in a sealed can.

2. 2-line ferrihydrite (FHYD II). An appropriate amount of ammonium hydroxide was added to 1 liter of 0.1 M $Fe(NO_3)_3 \cdot 9H_2O$ solution to bring the pH to 10. The reddish brown precipitate was filtered and washed until the pH decreased to 7. The cake was then oven-dried at 50°C and ground into a fine powder.

3. 2-line ferrihydrite (FHYD III). This sample was prepared using the method of Schwertmann and Cornell (1991) by adding 40 g of $Fe(NO_3)_3 \cdot 9H_2O$ to 0.5 liter water and adding KOH to the solution to bring the pH to 7–8. After centrifugation, the precipitate was dialyzed to remove electrolyte and subsequently freeze-dried.

4. 6-line ferrihydrite (6-L FHYD). The method of Schwertmann and Cornell (1991) was followed by adding 20 g of $Fe(NO_3)_3 \cdot 9H_2O$ into 2 liters of water preheated to 75°C. The solution was kept at 75°C for 10 to 12 minutes and then cooled rapidly. The solution was subsequently transferred to a dialysis bag and dialyzed for three days. The suspension was freeze-dried.

5. Al chemisorbed ferrihydrite (Al/FHYD). $Al(NO_3)_3 \cdot 9H_2O$ was added to a 0.1 M $Fe(NO_3)_3 \cdot 9H_2O$ solution with an atomic ratio of Al:Fe = 0.05. Ammonium hydroxide was then poured into the solution to bring the pH to 10. After washing and drying at 50°C, the sample was ground into fine powder.

6. Si chemisorbed ferrihydrite (Si/FHYD). Na_2SiO_3 was added to a 0.1 M $Fe(NO_3)_3 \cdot 9H_2O$ solution at an atomic ratio of Si:Fe = 0.05. The rest of the procedure is the same as that for Al/FHYD.

Experimental techniques

Mössbauer spectra were recorded using a constant acceleration spectrometer. The radioactive source consists of ~50 mCi of ^{57}Co in a Pd matrix. Because of the small particle size, Mössbauer spectra for ferrihydrite exhibit significant superparamagnetic relaxation effect (Ganguly *et al* 1993). In order to observe the magnetic splitting, all spectra were recorded at 12 K with an Air Products Displex cryogenic system.

Powder X-ray diffraction (XRD) was performed on an automated Rigaku Dmax X-ray diffractometer at a scanning speed of 1° (2θ)/min with Ni-filtered Cu Kα radiation, a 1° divergence slit, and a 0.6 mm receiving slit. Powder samples were mounted on glass slides. Small amount of grease was applied to the slide surface to hold the sample powder.

Transmission electron micrographs (TEM) were obtained with a Hitachi H800 NA scanning transmission electron microscope (STEM). Samples for TEM were prepared by suspending the catalysts in ethyl alcohol (weight ratio of alcohol to sample ~1000), to form a slightly turbid suspension. This suspension was constantly agitated in an ultrasonic bath for about an hour. A drop of the well-mixed suspension was carefully placed with a syringe on a thin carbon formvar film (Ted Pella, Inc., Redding, CA) pre-deposited on 200-mesh copper grids. The specimen was placed in a STEM sample holder after the alcohol had evaporated, leaving the particles on the grid.

Iron K-edge X-ray absorption fine structure (XAFS) measurements were performed at the National Synchrotron Light Source (NSLS) at beam line X-19A at Brookhaven National Laboratory. The radiation was monochromatized with a Si(111) double crystal monochromator with energy resolution of ~1 eV at the Fe K-edge. The monochromater was detuned by 60% to reduce the harmonic contents. The data were collected in the transmission mode with two ion chambers for recording I and I_o. The X-ray energy was varied from 100 eV below to 1000 eV above the Fe K-edge. The Fe K-edge (7112 eV) is defined as the first maximum in the derivative of the X-ray near edge absorption structure (XANES) spectrum for α-Fe metal. The XANES region (between −10 eV below the edge and 50 eV above the edge) was recorded in 0.2 eV steps.

Samples for the XAFS measurements were prepared by uniformly spreading the fine sample powder on a piece of thin tissue paper and then sealing with Scotch tape. Precautions were taken to minimize the thickness effects which can cause distortion of the XAFS spectrum (Heald 1988). In particular, a thick sample can causes erroneous increase of the pre-edge peak height,

https://doi.org/10.1346/CCMN.1994.0420610 Published online by Cambridge University Press

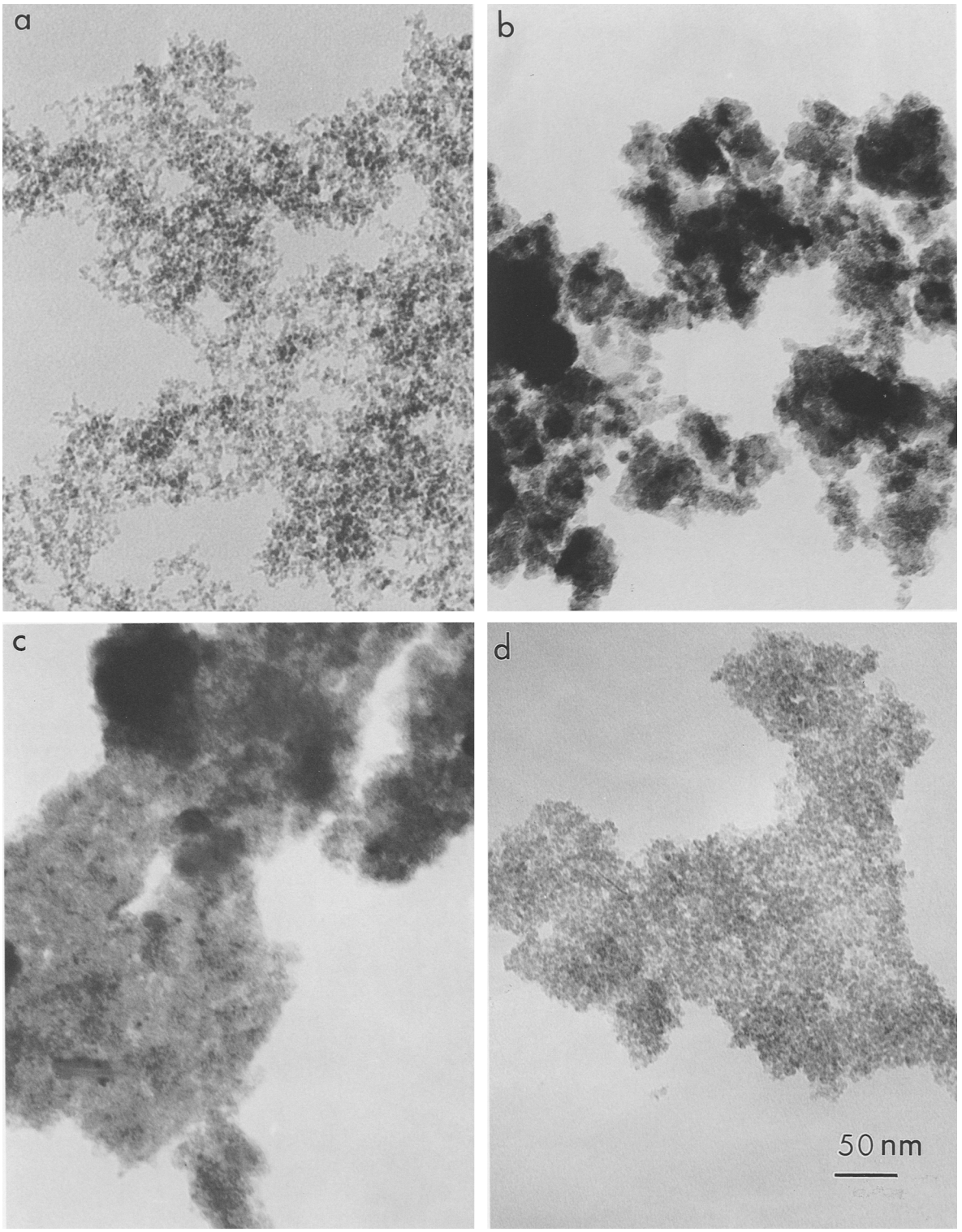


Figure 1. Electron micrographs of: (a) as-received ferrihydrite catalyst (FHYD I); (b) oven-dried 2-line ferrihydrite (FHYD II); (c) freeze dried 2-line ferrihydrite (FHYD III); (d) freeze dried 6-line ferrihydrite (6-L FHYD).

https://doi.org/10.1346/CCMN.1994.0420610 Published online by Cambridge University Press

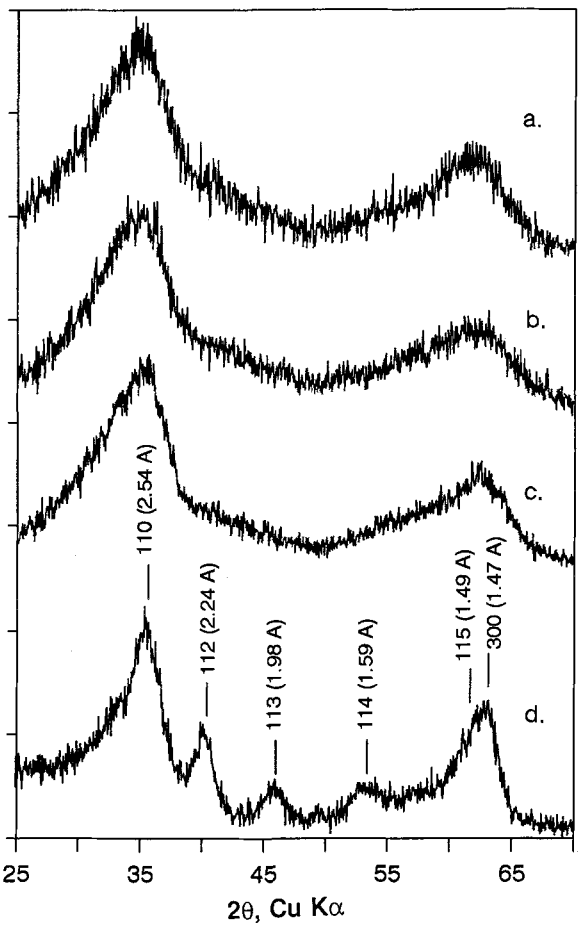


Figure 2. XRD patterns for: (a) as-received ferrihydrite catalyst (FHYD I); (b) oven-dried 2-line ferrihydrite (FHYD II); (c) freeze dried 2-line ferrihydrite (FHYD III); (d) freeze dried 6-line ferrihydrite (6-L FHYD), with hkl indices and d-spaces (in parentheses) labeled for the diffraction peaks.

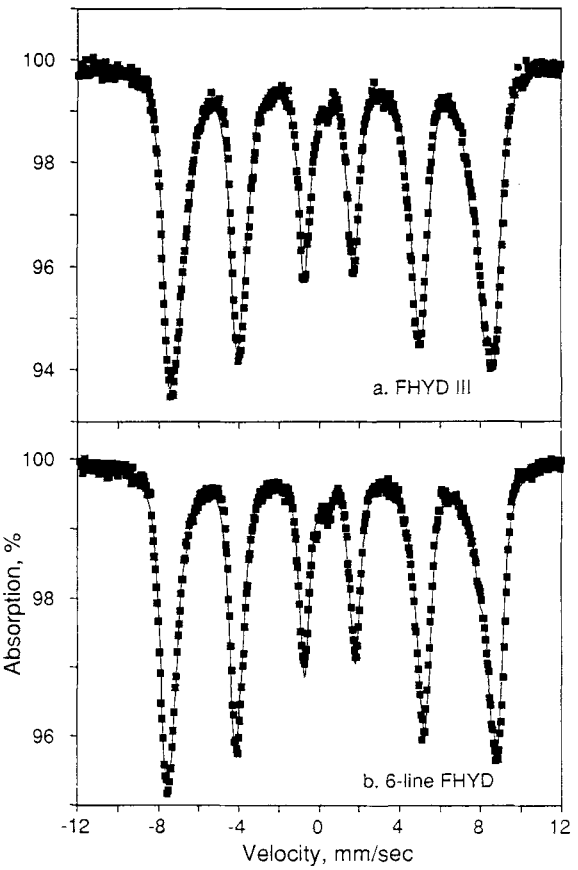


Figure 3. Mössbauer spectra recorded at 12 K for: (a) freeze-dried 2-line ferrihydrite (FHYD III); and (b) freeze-dried 6-line ferrihydrite (6-L FHYD).

a crucial parameter for this work. For each sample, several samples with different thickness were prepared for the XAFS measurements. Only the spectra with negligible thickness effects were chosen for detailed analysis. All spectra were collected at liquid-nitrogen temperature to reduce the thermal structural disorder. Standard procedures were employed to process and analyze the XAFS spectra (Sayers and Bunker 1988).

RESULTS AND DISCUSSION

Morphology of the samples

Figure 1 shows the electron micrographs of four ferrihydrite samples. The small particles in the two laboratory-synthesized 2-line ferrihydrites (FHYD II and FHYD III) are heavily aggregated as compared with those in the commercial ferrihydrite (FHYD I), which explains why the bulk densities of FHYD II and FHYD III are ten times that of FHYD I. The commercial FHYD I is formed at 500°C in a moisture-free environment (Rudy and Goodson 1991), which results in much less particle aggregation. Its Mössbauer spectra recorded at temperatures above 55 K exhibit a negligibly small value of recoilless fraction because of the free motion of the small particles (Ganguly *et al* 1994). In contrast, no significant reduction of the Mössbauer recoilless fraction was observed for FHYD II and FHYD III. As will be discussed in detail later, the particle aggregation in FHYD II and FHYD III is caused by the water molecules chemisorbed at the surface. These water molecules link small particles to form particle aggregates, preventing free motion of the small particles.

Structural characterization

The XRD results for the three 2-line ferrihydrites and the 6-line ferrihydrite show typical 2-line and 6-line patterns (Figure 2). The hkl indices for the 6-line ferrihydrite are labeled according to Schwertmann and Cornell (1991).

Mössbauer spectra collected at 12 K for FHYD III

https://doi.org/10.1346/CCMN.1994.0420610 Published online by Cambridge University Press

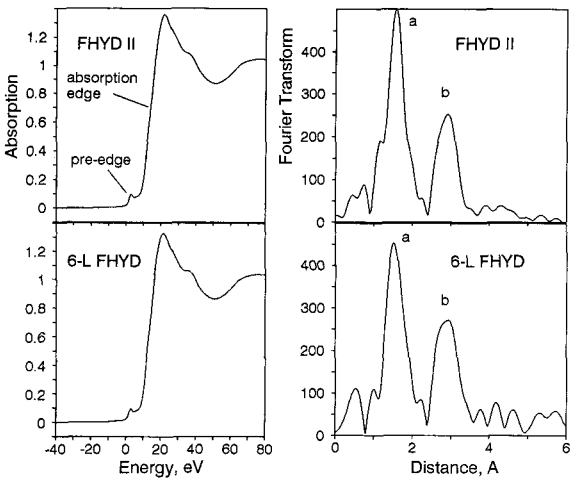


Figure 4. XANES (left) and the Fourier transforms of EXAFS (right) for oven-dried FHYD II and freeze-dried 6-L FHYD.

and 6-L FHYD show broad absorption peaks (Figure 3), indicating a distribution of magnetic hyperfine fields (Schwertmann and Cornell 1991) which probably arise from the different environments for the interior and the surface iron ions. The magnetic hyperfine fields at the nucleus of the surface iron ion are usually smaller than those in the interior of the particles (Van der Kraan 1973).

The X-ray near edge structure (XANES) spectra for both FHYD II and 6-L FHYD (Figure 4) are similar to those for oxyhydroxides (α-FeOOH and γ-FeOOH), indicating that the iron ions are coordinated by six oxygen/hydroxyl groups (Zhao *et al* 1993). The Fourier transforms of the EXAFS spectra (not corrected for phase shift) are dominated by two peaks at ~1.6 Å (peak a in Figure 4) and 2.8 Å (peak b), representing the nearest O/OH shell at ~2.0 Å and an Fe shell(s) at 3.0–3.2 Å, respectively (Zhao *et al* 1993). The structural parameters obtained from least-squares fitting of the inverse transforms are listed in Table 1. Details of the fitting procedure were previously reported (Zhao *et al* 1993). The coordination numbers for the first O/OH shell ($N_{O/OH}$) of the ferrihydrite samples are found to be ~5.4, in agreement with those for oxyhydroxids ($N_{O/OH}$ = 6) within the uncertainty ($\Delta N/N = \pm 20\%$) of EXAFS analysis. The intensity of the second peak at 2.8 Å (Figure 4) is weaker than those observed in oxyhydroxides (Zhao *et al* 1993), corresponding to a small coordination number (N_{Fe}) of 2–3 at 3.00–3.15 Å, as compared with N_{Fe} = 8 at 3.0–3.42 Å for α-FeOOH. The small N_{Fe} is attributed mainly to the fact that the iron ions at the surface have fewer iron neighbors. As the particle size decreases, the surface fraction increases, resulting in a smaller average coordination number. It is noted that peak b for 6-L FHYD is higher than that for FHYD II (Figure 4).

Table 1. Structural parameters obtained from EXAFS least-squares fittings for the ferrihydrite samples.

	Nearest O/OH shell			Fe shell(s)		
	R, Å (±1%)	N (±20%)	$\Delta\sigma^2$ [1]	R, Å	N	$\Delta\sigma^2$
FHYD I	1.99	5.5	0.0011	3.01	1.4	0.0008
				3.12	0.6	−0.0022
FHYD II	1.99	5.4	0.0008	3.00	2.0	0.0013
				3.14	1.1	−0.0018
FHYD III	1.98	5.2	0.0008	3.01	1.5	0.0009
				3.15	0.9	−0.002
6-L FHYD	1.98	5.2	0.0005	2.99	2.3	0.0013
				3.14	1.3	−0.0018

[1] $\Delta\sigma^2$ is the difference between the Debye-Waller coefficients of the samples and γ-FeOOH (Zhao *et al* 1993).

Least-squares fitting yields a coordination number of 3.6 as compared with 2.0–3.1 for the three 2-line ferrihydrite samples (Table 1), an indication of larger particle size.

XAFS pre-edge structures

The XAFS spectra for iron oxides usually exhibit a small pre-edge peak below the absorption edge (Figure 4), which is assigned to 1s → 3d transitions (Shulman *et al* 1976). The intensity of the transitions is represented by the peak areas, which is determined by multiplying the peak height by the peak width at ½ height after subtracting the background, i.e., the rising part of absorption edge. The heights of the peaks were normalized with respect to the edge step height (Sayers and Bunker 1988). The pre-edge peak area is very sensitive to the coordination symmetry; for iron ions with 6, 5, and 4 coordination, the ratio of the peak areas was found to be 1:2:3 (Roe *et al* 1984). Therefore, an increase of the pre-edge peak area over that for a compound with octahedral symmetry is an indication of the presence of lower coordination sites. For example, magnetite consists of 33% tetrahedral sites and 67% octahedral sites; hence, the contribution from the tetrahedral sites to the total peak area is $A_{tetr} = 0.33 \times 3 = 1$, and from the octahedral sites $A_{oct} = 0.67 \times 1 = 0.67$, and total area $A_{tot} = A_{tetr} + A_{oct} = 1.67$, a 67% increase over that for goethite or hematite ($A_{tot} = 1.00 \times 1 = 1$). XAFS pre-edges for goethite, magnetite, 6-L FHYD, and three 2-line ferrihydrites are shown in Figure 5. The pre-edge peaks were fitted with three Lorentzian peaks and an arctangent curve representing the absorption edge. The first two Lorentzian peaks are assigned to the 1s → 3d transition. The origin of the third one is not known. The total areas of the two 1s → 3d peaks for the samples are listed in Table 2. For the dried ferrihydrite samples, the peak areas are found to be between 0.116 to 0.137 units, which are significantly larger than those for goethite (A = 0.077 unit) and hematite (A = 0.074 unit), and close to that for

https://doi.org/10.1346/CCMN.1994.0420610 Published online by Cambridge University Press

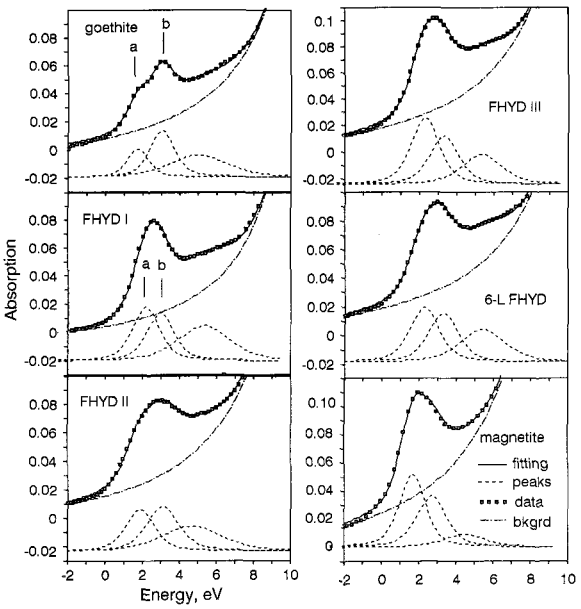


Figure 5. XAFS pre-edge peaks for: α-FeOOH (goethite), as-received FHYD I, oven-dried FHYD II, freeze- and vacuum-dried FHYD III, freeze-dried 6-L FHYD, and Fe_3O_4 (magnetite).

magnetite (A = 0.141 unit), indicating the presence of lower coordination sites in the materials. The variation of peak areas for the above samples can be seen in Figure 5.

Figure 5 also shows that for goethite, the two 1s → 3d peaks (a, b) are well resolved; whereas for the four ferrihydrite samples, only a broad single peak is observed, similar to that of magnetite. The d orbitals for the metal ions in transition metal compounds split into e_g and t_{2g} levels in an octahedral crystal field or t_2 and e levels in a tetrahedral crystal field. For oxygen ligands, the splitting of the e_g and t_{2g} levels is Δ_{oct} = 1.5 eV, and the splitting of the t_2 and e levels is $\Delta_{tetr} = (4/9) \times \Delta_{oct}$ = 0.7 eV (Marfunin, 1974). For iron oxides and oxyhydroxides with only octahedral coordination, the splitting of the e_g and t_{2g} levels can be seen in the spectra (Figure 5 for goethite). For magnetite, however, with 33% iron at tetrahedral sites and 67% iron at octahedral sites, the pre-edge should consist of four peaks. Due to the limited energy resolution at the Fe K-edge (~1 eV), only a single broad peak is seen (Figure 5). The pre-edge was also fitted with three Lorentzian peaks plus an arctangent curve and the first two peaks are assigned to the 1s → 3d transitions. The splitting of the first two peaks is found to be ~1 eV. The pre-edge peaks for the ferrihydrite samples all show a single peak pattern, resembling that for magnetite (Figure 5) and two-peak fitting yields a similar splitting of ~1 eV. From the peak areas, it is estimated that the ferrihydrite samples consist of 20–30% tetrahedral sites, assuming

Table 2. XAFS pre-edge peak areas for the ferrihydrite samples and model compounds.

Sample	Preparation condition	Area (A), pre-edge ($\Delta A = \pm 0.01$)
Fe_3O_4	lab synthesized	0.141
FHYD I	as-received	0.127
	moist air exposed	0.110
FHYD II	cake	0.091
	oven-dried (50°C)	0.116
FHYD III	freeze-dried	0.112
	freeze- and vacuum-dried	0.137
6-L FHYD	freeze-dried	0.118
	freeze- and vacuum-dried	0.122
Si/FHYD	vacuum-dried	0.119
Al/FHYD	vacuum-dried	0.124
α-FeOOH	lab synthesized	0.077
α-Fe_2O_3	lab synthesized	0.074

that the increase of the pre-edge peak area is due to the presence of tetrahedral sites only. However, it should be noted that those sites with three or five coordination would have similar effects.

The presence of lower coordination sites in the ferrihydrite samples appears to contradict their XANES spectra (Figure 4) which resemble the spectra of octahedrally coordinated α-FeOOH and γ-FeOOH (Zhao *et al* 1993). If there were lower coordination sites, the XANES spectra are expected to show significant changes, as can be seen in the XANES spectra for magnetite and maghemite (Zhao *et al* 1993). However, it is noted that XANES spectrum is the result of multiple-scattering between the central absorbing atom and its neighboring coordination shells. Theoretical calculations by Greaves et al. (1981) demonstrate that the full XANES features only emerge when the multiple-scattering calculation includes more than three coordination shells for fcc copper. Therefore, XANES is basically a *bulk effect* and the surface iron ions will not significantly contribute to the XANES spectra because they have one complete O/OH shell only. Therefore, we conclude that, instead of being uniformly distributed in the ferrihydrite structure, the lower coordination sites indicated by the XAFS pre-edge spectra are predominantly at the ferrihydrite surface.

Mössbauer spectroscopy represents a second technique for identifying iron in the lower coordination sites. The interpretation of Mössbauer spectra for ferrihydrite, however, is still controversial. Recently, Pankhurst and Pollard (1992) reported Mössbauer spectra for 2-line and 6-line ferrihydrites at 4.2 K and with external magnetic fields from zero to 9 T. For both samples, the Mössbauer spectra exhibit very symmetric absorption lines and, as the external field increases, the spectra split into two sets of six-line magnetic components, although the two sextets for the 6-line ferrihydrite are less resolved and the spectrum was fitted with one sextet by the authors. Because the spec-

https://doi.org/10.1346/CCMN.1994.0420610 Published online by Cambridge University Press

trum for the 2-line ferrihydrite is very symmetric, a single value of isomer shift (δ = 0.48 mm/s) was used by Pankhurst and Pollard (1992) to fit the spectra and the quadruple splittings (Δ) for the two sextets were found to be equal within their uncertainties (no specific data were given by Pankhurst and Pollard 1992). The δ and Δ values obtained for the two sextets are characteristic of the octahedrally coordinated Fe(III) at liquid helium temperature. These results are very different from those for bulk Fe_3O_4 and γ-Fe_2O_3. The spectra for bulk Fe_3O_4 and γ-Fe_2O_3 are asymmetric with zero field and the asymmetry becomes more pronounced with an applied field, because the δ and Δ values for the tetrahedral Fe(II, III) sites are significantly different from those for the octahedral Fe(III) sites (Amstrong *et al* 1966; Hargrove and Kündig 1970). Based on the above observation, Pankhurst and Pollard (1992) concluded that iron ions in ferrihydrite are exclusively octahedrally coordinated.

However, it is more appropriate to compare the Mössbauer spectra for ferrihydrite with those for *small particle* rather than *bulk* Fe_3O_4 or γ-Fe_2O_3. A literature survey indicates that as the particle sizes of Fe_3O_4 and γ-Fe_2O_3 decrease, the Mössbauer spectra indeed do become more symmetric. Examples can be found in publications by Mørup (1983) for a 60 Å Fe_3O_4 particle sample at 78 K, by McNab *et al* (1968) for a 100 Å Fe_3O_4 particle sample at temperatures from 4.2 to 300 K and with a zero or 0.2 T applied field, and by Morrish *et al* (1976) and Haneda and Morrish (1977) for a 100 Å γ-Fe_2O_3 particle sample at 4.2 K and with a 5 T applied field. The symmetry in the spectra would certainly cause the values of isomer shift and quadruple splitting for the two magnetic components to become less distinguishable. In particular, it is worthwhile to compare the spectra for the 100 Å γ-Fe_2O_3 particle sample by Haneda and Morrish (1977, Figures 1 and 3) with the spectrum by Pankhurst and Pollard (1992, Figure 1), since the experimental conditions are similar. Both samples show symmetric absorption lines and two sextets. The differences in the spectra are mainly due to the fact that the particles in ferrihydrite are much smaller. Given that the particle size of the γ-Fe_2O_3 sample is 100 Å, one would expect that as the particle size decreases, the spectra will show broader and more symmetric lines (McNab *et al* 1968), and enhanced $\Delta m_I = 0$ lines (the second and fifth lines) (Morrish *et al* 1976). Therefore, from the Mössbauer spectra reported by Pankhurst and Pollard (1992), one can not rule out the possibility of the presence of tetrahedral sites in ferrihydrites.

XAFS spectra were also collected for ferrihydrite samples prepared with different surface water contents. Analysis of the XAFS pre-edge peaks (Table 2) shows a clear pattern: the drier the sample, the larger the pre-edge peak area. The variation of the peak areas can be seen in Figure 6. The results reveal that some surface

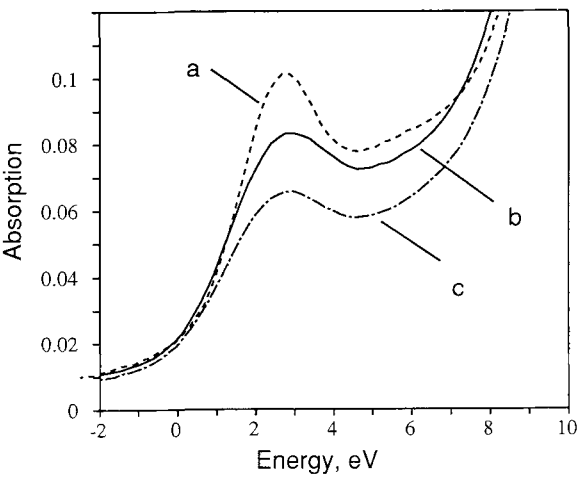


Figure 6. XAFS pre-edge peaks of the ferrihydrite samples prepared with various drying conditions: (a) FHYD III, freeze- and vacuum-dried; (b) FHYD III, freeze-dried; (c) FHYD II, cake after washing and filtering.

iron ions become coordination unsaturated (CUS) as a result of dehydroxylation.

It is noted that the pre-edge peak area for the ferrihydrite cake (A = 0.091, Table 2) is quite close to those for goethite (A = 0.077) and hematite (A = 0.074). Since the ratio of the peak areas for iron ions with 6, 5, and 4 coordination is 1:2:3 (Roe *et al* 1984), a value of 0.091 for A corresponds to 90% of octahedral sites and 10% tetrahedral sites, suggesting that before drying, the iron ions in ferrihydrite are predominantly six-fold coordinated. Previously, Manceau *et al* (1990) reported that the heights (not the areas) of the pre-edge peaks for their 2-line and 6-line ferrihydrites are comparable to those for hematite and goethite, which allowed them to rule out the possibility of the presence of tetrahedral sites claimed by Eggleton and Fitzpatrick (1988). Although no details of sample preparation were given, Manceau *et al* (1990) did mention that "most authors agree that iron ions are exclusively 6-fold coordinated in solutions and ferric gels." It would appear that the surface tetrahedral sites are increasingly formed as ferrihydrite evolves from a hydrogel state to an anhydrous state.

For the 6-line ferrihydrite, further drying at 130°C in vacuum after freeze drying increases the pre-edge peak area from 0.118 to 0.122 (Table 2), suggesting that limited dehydroxylation has taken place. From the present data, it is not clear whether CUS sites are present at the 6-line ferrihydrite surface.

Effects of chemisorbed impurity anions on phase transformation

When impurity anions (M) are present in the precipitation solution, the ferrihydrite precipitate may adsorb the impurity anions to form a Fe-O-M surface

https://doi.org/10.1346/CCMN.1994.0420610 Published online by Cambridge University Press

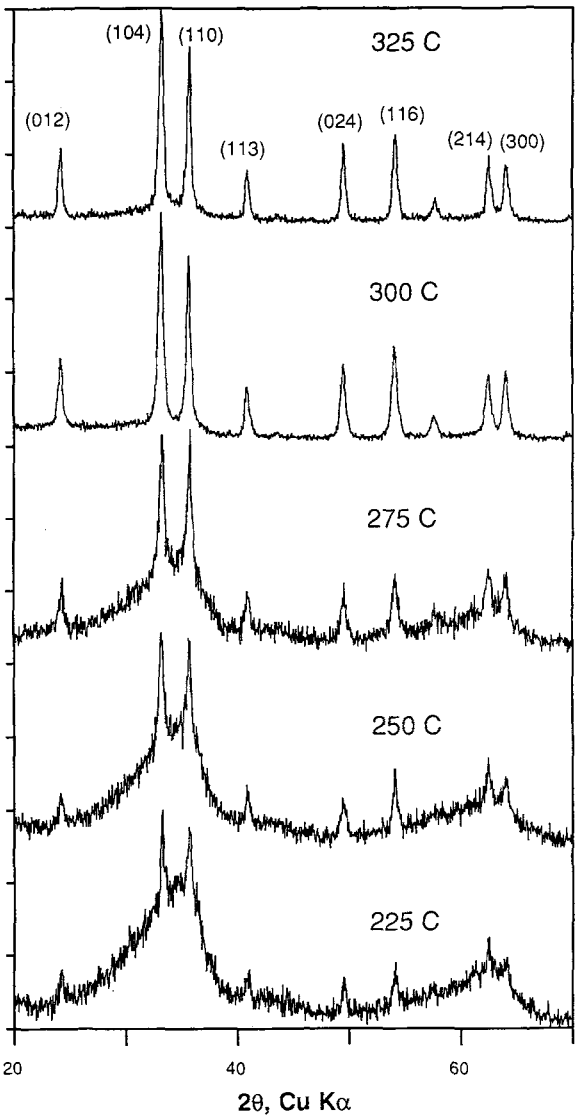


Figure 7. XRD patterns for FHYD I after annealing at various temperatures for 5 hours in air.

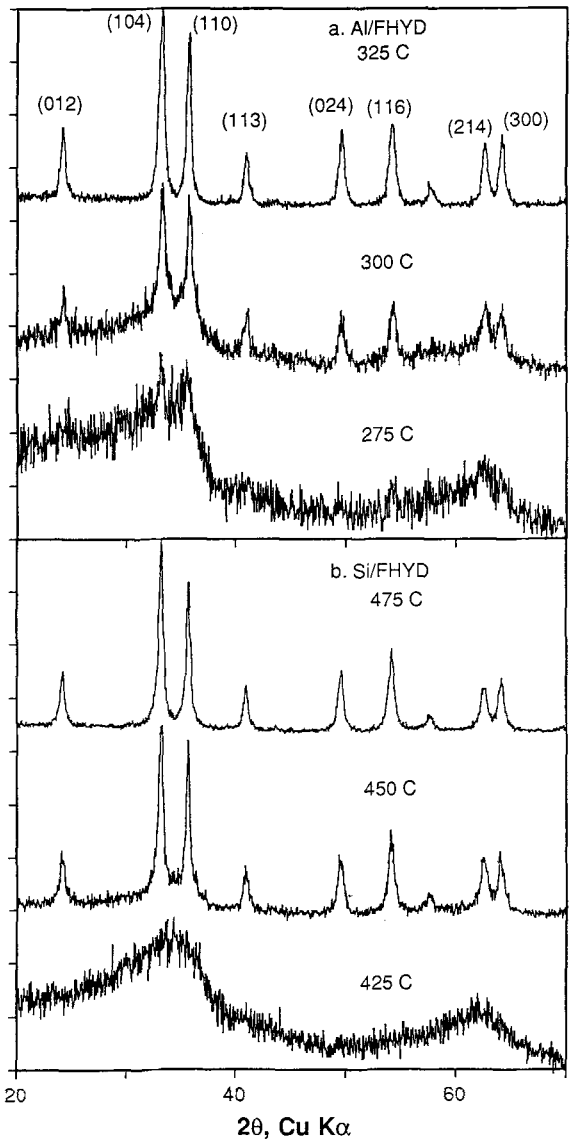


Figure 8. XRD patterns for Al/FHYD and Si/FHYD after annealing at various temperatures for 5 hours in air.

layer (Waychunas *et al* 1993; Zhao *et al* 1994). To examine the effects of the Fe-O-M layer on the phase transformation of ferrihydrite to hematite, two ferrihydrite samples chemisorbed with Si (Si/FHYD) and Al (Al/FHYD) were prepared. The two samples and a pure ferrihydrite (FHYD I) were annealed in a furnace at temperatures from 200°C to 500°C for 5 hours in air and XRD measurements were subsequently taken (Figures 7, 8). Before annealing, the XRD patterns for Al/FHYD and Si/FHYD show two broad peaks and the XAFS pre-edge peak areas are found to be 0.119 and 0.124 units, respectively, similar to those for FHYD I (Figure 2, Table 2). After annealing at 225°C, the XRD pattern for FHYD I shows traces of crystalline hematite, as indicated by the sharp diffraction peaks superimposed on two broad ferrihydrite peaks (Figure 7). The d-spaces for the diffraction peaks for the 325°C annealed ferrihydrite sample are listed in Table 3. The percentage of α-Fe_2O_3 increases with annealing temperatures and after annealing at 300°C, only α-Fe_2O_3 is seen. For Al/FHYD and Si/FHYD, however, XRD peaks for α-Fe_2O_3 emerge at higher temperatures of 275°C and 425°C, and the phase transformations are completed more abruptly at 300°C and 450°C, respectively (Figure 8).

These phenomena are expected from the proposed structural model for ferrihydrite (Zhao *et al* 1993). Being coordination unsaturated, the CUS sites at the surface can easily absorb water molecules to fill the CUS

https://doi.org/10.1346/CCMN.1994.0420610 Published online by Cambridge University Press

Table 3. Powder X-ray diffraction data for FHYD I after annealing at 325°C for 5 hours.

2θ (°)	(hkl)	d-space (Å)	Intensity (relative)
24.15	012	3.681	38
33.15	104	2.700	100
35.65	110	2.516	81
40.85	113	2.207	26
49.45	024	1.842	41
54.10	116	1.694	45
62.45	214	1.486	28
64.05	300	1.453	29

sites. These surface water molecules link the small ferrihydrite particles to form particle aggregates, and at elevated temperatures, these water molecules evolve from the particle contacts, causing particles to agglomerate and transform to hematite (Feng *et al* 1993). Therefore, the transformation rate depends on the coverage of water molecules at the surface as well as temperature. Even at room temperature, as noted by Schwertmann and Cornell (1991), the formation of hematite can take place slowly. Since the formation of hematite occurs only from those ferrihydrite particles linked by chemisorbed water molecules, both ferrihydrite and hematite are observed at low temperatures (Figure 7). At higher temperatures (>300°C), however, the phase transformation is caused by dehydroxylation taking place in the interior of the particles and these dehydroxylated particles quickly agglomerate to form larger hematite particles. Therefore, one may view the CUS sites with chemisorbed water molecules as the crystal growth sites at low temperatures. However, when impurity anions are present in the precipitation solution, the CUS sites may favorably adsorb the impurity anions to form a Fe-O-M layer, thereby blocking the crystal growth sites. For Si/FHYD with Si/Fe = 5%, assuming 30% of the iron ions are at the surface and most of them are coordination unsaturated, because a SiO_4^{-4} may occupy three CUS sites, 5% Si will block most of the crystal growth sites.

The adsorbed impurity anions may inhibit the formation of hematite in three ways: (i) At low temperatures, because the CUS sites are occupied by impurity anions, the formation of hematite induced by chemisorbed water molecules will not take place; (ii) The surface Fe-O-M layer may prevent the small particles from dehydroxylation at high temperatures; and (iii) Even after dehydroxylation, the surface Fe-O-M layer inhibits the agglomeration of small particles because of incompatibility of the impurity ions and iron ions. Consequently, the formation of hematite will take place at higher temperatures and the phase transition temperature will depend on the nature and the coverage of the impurity anions. Si is much more effective than Al in inhibiting the formation of hematite because Si favors a tetrahedral symmetry, which is incompatible with either goethite or hematite. Hence, with Si absorbed at the ferrihydrite surface, crystal growth leading to the formation of hematite is retarded. On the other hand, AlOOH and Al_2O_3 are isostructural with goethite and hematite, and Al will readily substitute for Fe in goethite or hematite to form solid solutions. As a result, Al is much less effective in retarding the phase transformation than Si. It is known that only 2% of Si can be incorporated into the goethite lattice (Quin *et al* 1988), while the substitution of Al for Fe in hematite and goethite can reach 15% and 30%, respectively (Schwertmann and Cornell 1991). Quin *et al* (1988) speculated that "the Si . . . must have been adsorbed strongly on crystal growth sites."

CONCLUSION

The presence of lower coordination sites in ferrihydrite is confirmed by XAFS analysis of ferrihydrite samples prepared over a range of precipitation and drying conditions. These sites, which are most likely tetrahedral, are formed as the material is evolved from a hydrogel state to an anhydrous state. Instead of uniformly distributing in the structure, the tetrahedral sites are at the surface, and they become coordination unsaturated as a result of dehydroxylation. This structural model provides a microscopic view of the phase transformation of ferrihydrite to hematite. With chemisorbed water molecules, the surface CUS sites become the crystal growth sites, responsible for the phase transformation at low temperature; on the other hand, when impurity anions are present in precipitation, the CUS sites may be filled with chemisorbed impurity anions, which in turns block the crystal growth sites, inhibiting the formation of hematite.

ACKNOWLEDGMENTS

The authors would like to thank Vikram Mahajan for his assistance in acquisition of the Mössbauer spectra. Financial support from the U.S. Department of Energy (contract No. DE-FC22-90PC90029) is gratefully acknowledged.

REFERENCES

Armstrong, R. J., A. H. Morrish, and G. A. Sawatzky. 1966. Mössbauer study of ferric ions in the tetrahedral and octahedral sites of a spinel. *Phys. Lett.* **23**: 414–416.

Cardile, C. M. 1988. Tetrahedral Fe^{3+} in ferrihydrite: ^{57}Fe Mössbauer spectroscopic evidence. *Clays & Clay Miner.* **36**: 537–539.

Cornell, R. M., and U. Schwertmann. 1979. Influence of organic anions on the crystallization of ferrihydrite. *Clays & Clay Miner.* **27**: 402–410.

Eggleton, R. A., and R. W. Fitzpatrick. 1988. New data and a revised structural model for ferrihydrite. *Clays & Clay Miner.* **36**: 111–124.

Feng, Z., J. Zhao, F. E. Huggins, and G. P. Huffman. 1993.

https://doi.org/10.1346/CCMN.1994.0420610 Published online by Cambridge University Press

Agglomeration and phase transition of a nanophase iron oxide catalyst. *J. Catal.* **143**: 510–519.

Fleischer, M., G. Y. Chao, and A. Kato. 1975. New mineral names. *Am. Mineral.* **60**: 485–486.

Fuller, C. C., J. A. Davis, and G. A. Waychunas. 1993. Surface chemistry of ferrihydrite: Part II. Kinetics of arsenate adsorption and coprecipitation. *Geochim. Cosmochim. Acta* **57**: 2271–2282.

Ganguly, B., F. E. Huggins, and Z. Feng, and G. P. Huffman. 1994. Anomalous recoilless fraction of 30 Å FeOOH particles. *Phys. Rev. B.* **49**: 3036–3042.

Ganguly, B., F. E. Huggins, K. R. P. M. Rao, and G. P. Huffman. 1993. Determination of the particle size distribution of iron oxide catalysts from superparamagnetic Mössbauer relaxation spectra. *J. Catal.* **142**: 552–560.

Greaves, G. N., P. J. Durham, G. Diaken, and P. Quin. 1981. Near-edge absorption spectra for metallic Cu and Mn. *Nature* **294**: 139–141.

Haneda, K., and A. H. Morrish. 1977. On the hyperfine field of γ-Fe_2O_3 small particles. *Phys. Lett.* **64A**: 259–262.

Hargrove, R. S., and W. Kündig. 1970. Mössbauer measurements of magnetite below the Verwey transition. *Solid State Comm.* **8**: 303–308.

Heald, S. M. 1988. Design of an EXAFS experiment. In *X-ray Absorption: Principles, Applications, Techniques of EXAFS, SEXAFS and XANES.* D. C. Koningsberger and R. Prins, eds. New York: John Wiley, 87–118.

Huffman G. P., B. Ganguly, J. Zhao, K. R. P. M. Rao, N. Shah, Z. Feng, F. E. Huggins, M. M. Taghiei, F. Lu, I. Wender, V. R. Pradhan, J. W. Tierney, M. M. Seehra, M. M. Ibrahim, J. Shabtai, and E. M. Eyring. 1993. Structure and dispersion of iron-based catalyst for direct coal liquefaction. *Energy Fuels* **7**: 285–296.

Johnston, J. H., and D. G. Lewis. 1983. A detailed study of the transformation of ferrihydrite to hematite in an aqueous medium at 92°C. *Geochem. Cosmochim. Acta* **47**: 1823–1831.

Karim, Z. 1984. Characterization of ferrihydrites formed by oxidation of $FeCl_2$ solutions containing different amounts of silica. *Clays & Clay Miner.* **32**: 181–184.

Knözinger, H., and P. Ratnasamy. 1978. Catalytic aluminas: Surface models and characterization of surface sites. *Catal. Rev.-Sci. Eng.* **17**: 31–70.

Liaw, B. J., D. S. Cheng, and B. L. Yang. 1989. Oxidative dehydrogenation of 1-butene on iron oxyhydroxides and hydrated iron oxides. *J. Catal.* **118**: 312–326.

Marfunin, A. S. 1974. *Physics of Minerals and Inorganic Materials.* New York: Springer-Verlag, 216–227.

Manceau, A., J.-M. Combes, and G. Calas. 1990. New data and a revised structural model for ferrihydrite. *Clays & Clay Miner.* **38**: 331–334.

McNab, T. K., R. A. Fox, and A. F. J. Boyle. 1968. Some magnetic properties of magnetite (Fe_3O_4) microcrystals. *J. Appl. Phys.* **39**: 5703–5711.

Morrish, A. H., K. Haneda, and P. J. Schurer. 1976. Surface magnetic structure of small γ-Fe_2O_3 particles. *J. de Physique* **C6**: 301–305.

Morup, S. 1983. Mössbauer spectroscopy studies of suspensions of Fe_3O_4 microcrystals. *J. Magn. Magn. Materials* **39**: 45–47.

Murad, E. 1988. The Mössbauer spectrum of "well"-crystallized ferrihydrite. *J. Magn. Magn. Materials* **74**: 153–157.

Pankhurst, Q. A., and R. J. Pollard. 1992. Structural and magnetic properties of ferrihydrite. *Clays & Clay Miner.* **40**: 268–272.

Quin, T. G., G. J. Long, C. G. Benson, S. Mann, and R. J. P. Williams. 1988. Influence of silicon and phosphorus on structural and magnetic properties of synthetic goethite and related oxides. *Clays & Clay Miner.* **36**: 165–175.

Roe, A. L., D. J. Schneider, R. J. Mayer, J. W. Pytz, J. Widom, and L. Que, Jr. 1984. X-ray absorption spectroscopy of iron-tyrosinate protein. *J. Am. Chem. Soc.* **106**: 1676–1681.

Rudy, T. P., and F. R. Goodson. 1991. Method for making iron oxide catalyst. U.S. Patent 5,047,382.

Russell, J. D. 1979. Infrared spectroscopy of ferrihydrite: Evidence for the presence of structural hydroxyl groups. *Clay Miner.* **14**: 109–113.

Sayers, D. E., and B. A. Bunker. 1988. Data analysis. In *X-ray Absorption: Principles, Applications, Techniques of EXAFS, SEXAFS and XANES.* D. C. Koningsberger and R. Prins, eds. New York: John Wiley, 211–256.

Schwertmann, U. and R. M. Cornell. 1991. *Iron Oxides in the Laboratory.* Weinheim: VCH, Weinheim City in Germany, 89–94.

Schwertmann, U., and H. Thalmann. 1979. The influence of [Fe(II):cb, {Si}, and pH on the formation of lepidocrocite and ferrihydrite during oxidation of aqueous $FeCl_2$ solution. *Clay Miner.* **11**: 189–200.

Shulman, R. G., Y. Yafet, P. Eisenberger, and W. E. Blumberg. 1976. Observation and interpretation of x-ray absorption edges in iron compounds and proteins. *Proc. Natl. Acad. Sci. USA,* **5**: 1384–1388.

Towe, K. M. and W. F. Bradley. 1967. Mineralogical constitution of colloidal "hydrous ferric oxides." *J. Colloid Interface Science* **24**: 383–392.

Van der Kraan, A. M. 1973. Mössbauer effect studies of surface ions of ultrafine α-Fe_2O_3 particles. *Phys. Stat. Sol.* **18**: 215–226.

Waychunas, G. A., B. A. Rea, C. C. Fuller, and J. A. Davis. 1993. Surface chemistry of ferrihydrite: Part I. EXAFS studies of the geometry of coprecipitated and adsorbed arsenate. *Geochim. Cosmochim. Acta* **57**: 2251–2269.

Zhao, J., Z. Feng, F. E. Huggins, N. Shah, G. P. Huffman, and I. Wender. 1994. Role of molybdenum at the iron oxide surface. *J. Catal.* **148**: 194–197.

Zhao, J., F. E. Huggins, Z. Feng, F. Lu, N. Shah, and G. P. Huffman. 1993. Structure of a nanophase iron oxide catalyst. *J. Catal.* **143**: 499–509.

Received 22 March 1994; accepted 27 June 1994; ms. 2483)

https://doi.org/10.1346/CCMN.1994.0420610 Published online by Cambridge University Press